The role of pseudospin in the optical and electronic properties of relativistic materials

John D. Malcolm

Ph.D. Thesis, University of Guelph

Supervisor: Prof. Elisabeth J. Nicol

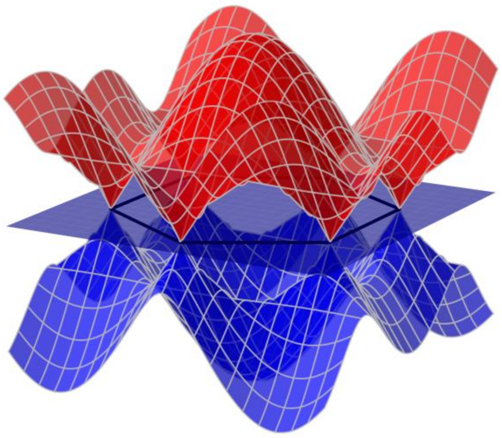

Motivation: Graphene

The hallmark 'relativistic material'

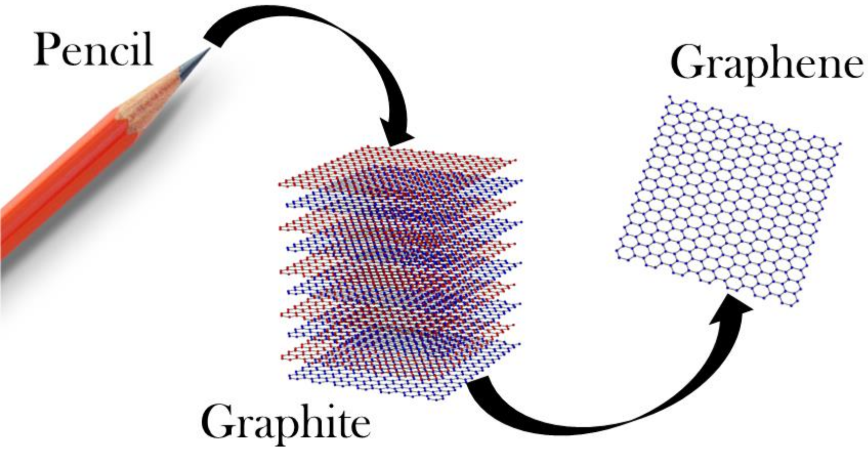

- Discovered in 2004 (2010 Nobel prize in physics)
- Incredible properties and high potential for technology
- Exhibits remarkable behaviour from a fundamental perspective

Can we find other relativistic materials similar to graphene?
What would their properties be? Experimental signatures?

Relativistic Condensed Matter

- At low energy, the quasiparticles in graphene are described by the two-dimensional massless Dirac-Weyl (DW) Hamiltonian, with an *emergent* SU(2) spin-1/2 called pseudospin
- This motivates the supposition of condensed matter systems with pseudospin higher than 1/2:

$$\hat{\mathcal{H}}(\boldsymbol{k}) = \hbar v \boldsymbol{\sigma} \cdot \boldsymbol{k} \rightarrow \hbar v \boldsymbol{S} \cdot \boldsymbol{k}$$

- The $\boldsymbol{\sigma}/2$ (spin-1/2 matrices) are replaced with the general spin-s matrices, $\boldsymbol{S}$. This leads to an energy spectrum depending on spin projections, λ,

$$\varepsilon_\lambda(k) = \lambda \hbar v k, \qquad \lambda = \{-s, -s+1, \dots s\}$$

Dirac-Weyl Dispersions

- Linear band dispersions that touch at a single point (the **Dirac point**).
- Integer pseudospin systems contain a completely **flat band**, placing a large density of states at exactly zero energy.
- Systems with psuedospin > 1 are host to nested Dirac cones.

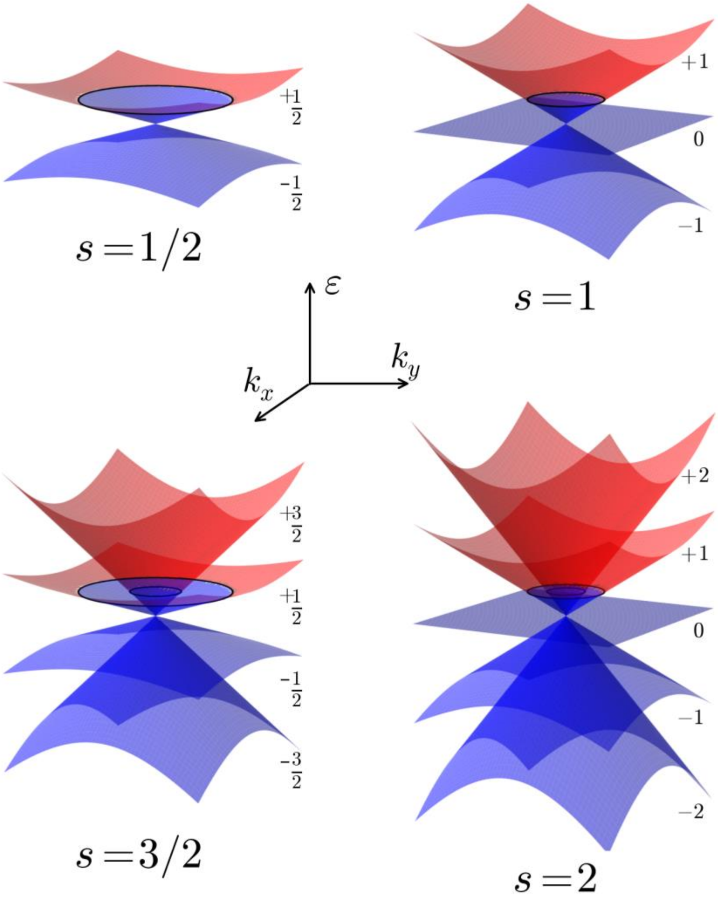

Dirac-Weyl Magneto-Optics

s=1

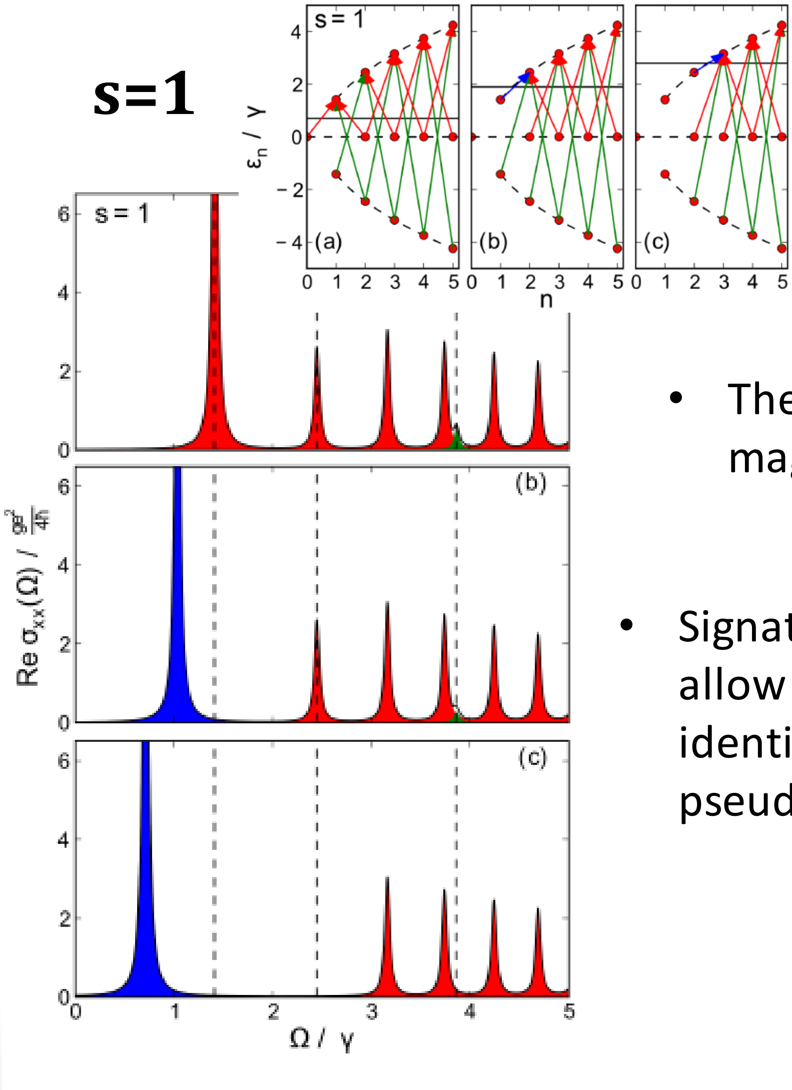

Phys. Rev. B **90**, 035405 (2014).

- Snowshoe diagrams show allowed optical transitions between Landau levels

- These diagrams help to explain features of magneto-optical conductivity

- Signatures in spectra allow for the potential identification of different pseudospin materials

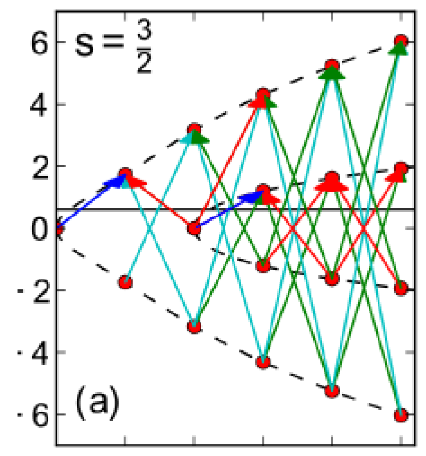

Kane Fermion Magneto-Optics

Phys. Rev. B **92**, 035118 (2015)
Phys. Rev. B **94**. 224305 (2016)

- Kane model applies to narrow-gap zinc-blende materials.
- Massless Kane fermions argued to be hybrid pseudospin-1/2 and 1.
- Used model to accurately match experimental optical conductivity of HgCdTe, which exhibits pseudospin-1 characteristics.

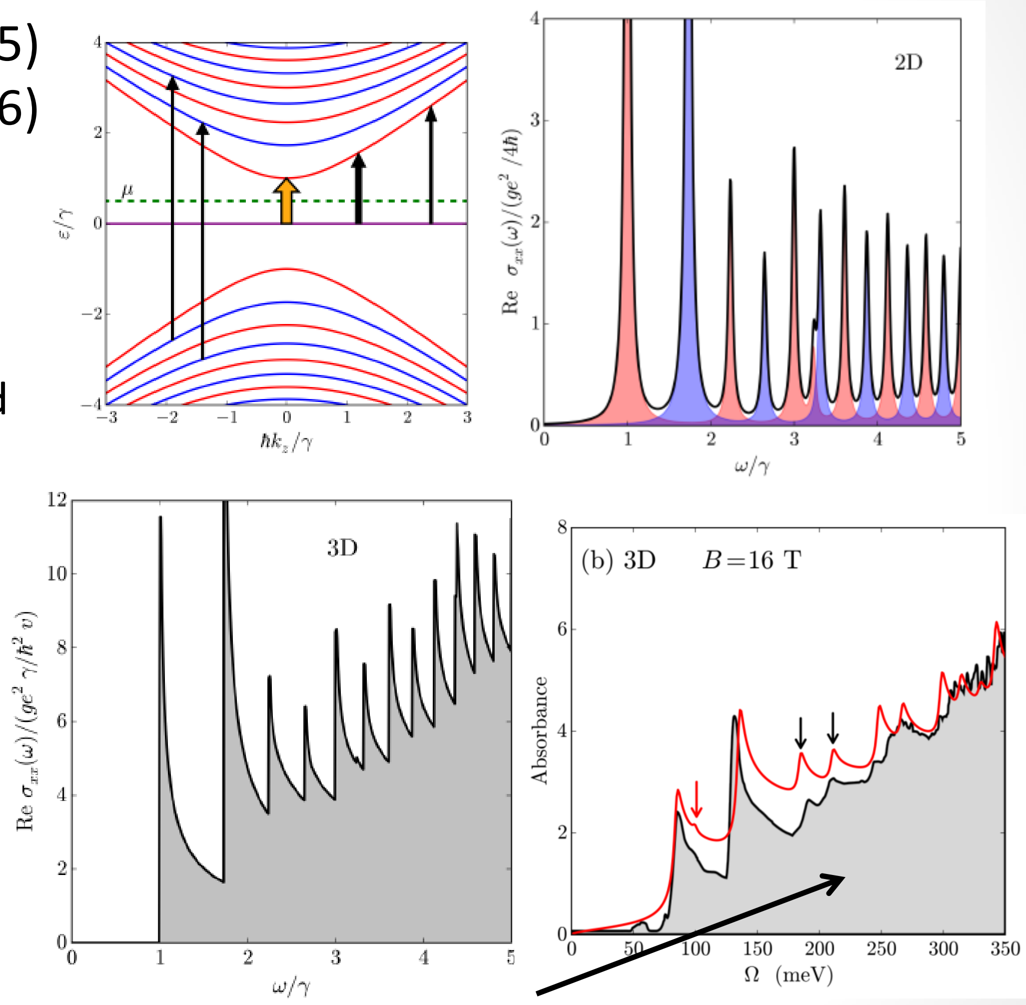

Experimental data from Orlita et al. Nat. Phys. **10**, 233 (2014)

Pseudospin-1 Polarizability

Phys. Rev. B **93**, 165433 (2016)

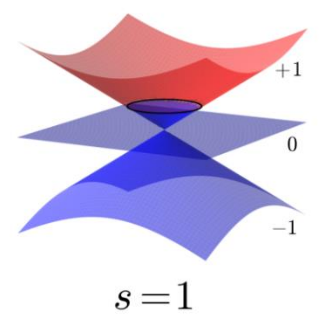

- Analytical derivation of polarizability, describing dielectric properties of pseudospin-1 materials.
- Along with many other phenomena, polarizability details plasmonic behaviour (collective charge oscillations).
- Flat band provides large screening effects.

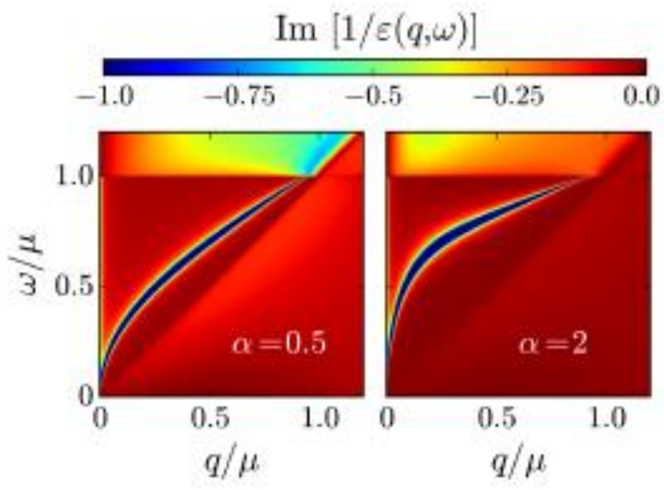

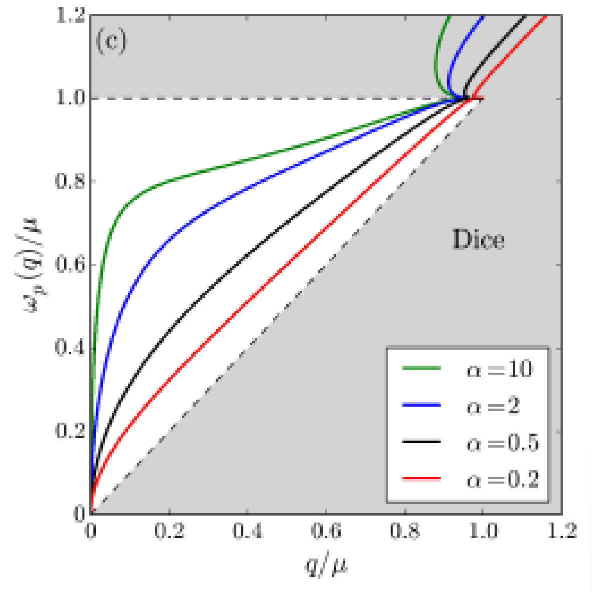

Thank You!

- J.D. Malcolm and E.J. Nicol, 'Magneto-optics of general pseudospin-*s* two-dimensional Dirac-Weyl fermions,' Phys. Rev. B **90**, 035405 (2014)
- J.D. Malcolm and E.J. Nicol, 'Magneto-optics of massless Kane fermions: Role of the flat band and unusual Berry phase,' Phys. Rev. B **92**, 035118 (2015)
- J.D. Malcolm and E.J. Nicol, 'Frequency-dependent polarizability, plasmons, and screening in the two-dimensional pseudospin-1 dice lattice,' Phys. Rev. B **93**, 165433 (2016)
- J.D. Malcolm and E.J. Nicol, 'Analytic evaluation of Kane fermion magneto-optics in two and three dimensions,' Phys. Rev. B **94**. 224305 (2016)

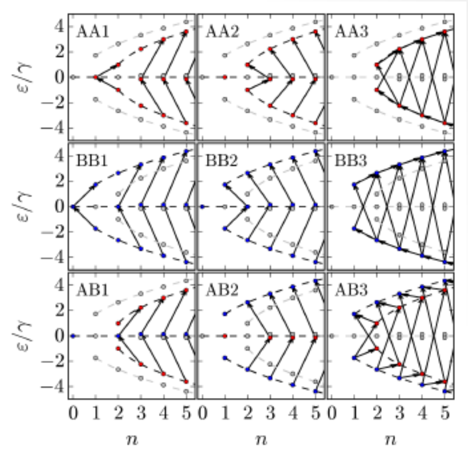

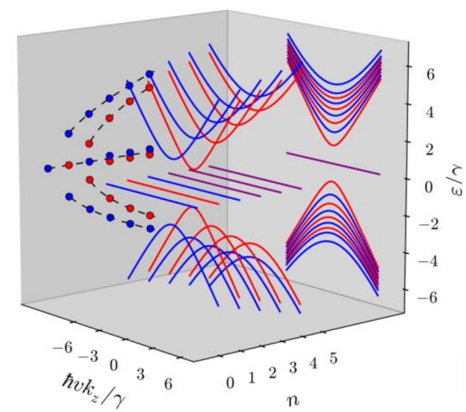

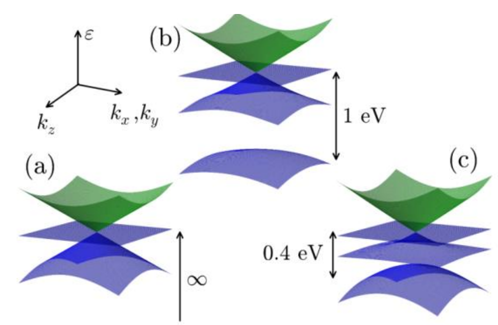

The Dice Lattice

An example of a toy lattice which gives rise to pseudospin-1 DW fermions.

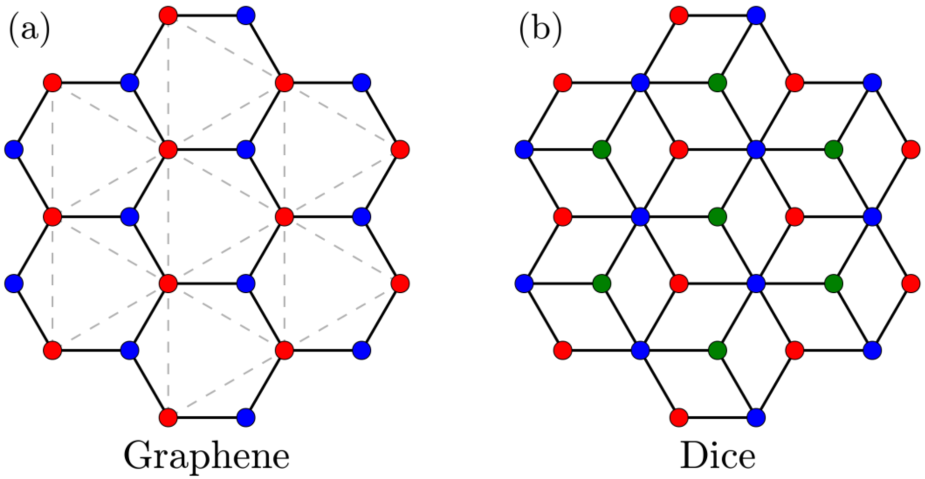

Tight-binding Hamiltonian:

$$\hat{\mathcal{H}} = t \sum_{<ij>} {c_i}^{\dagger} c_j$$

Diagonalize for energy dispersion:

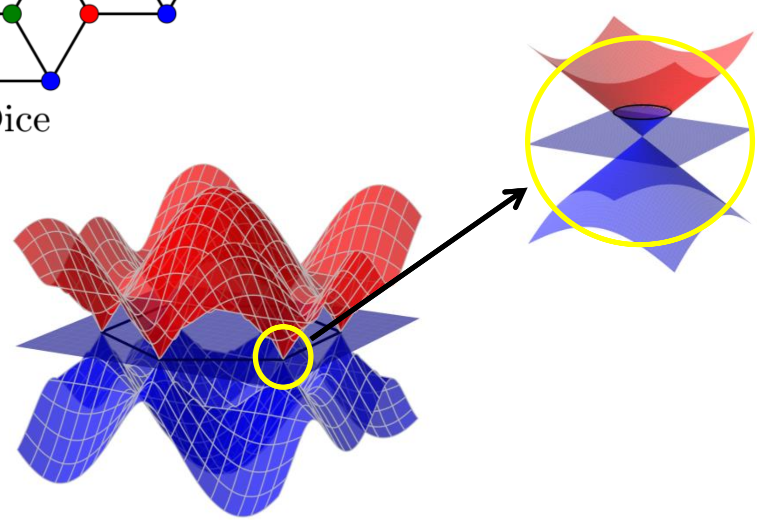

The α-T_3 Model

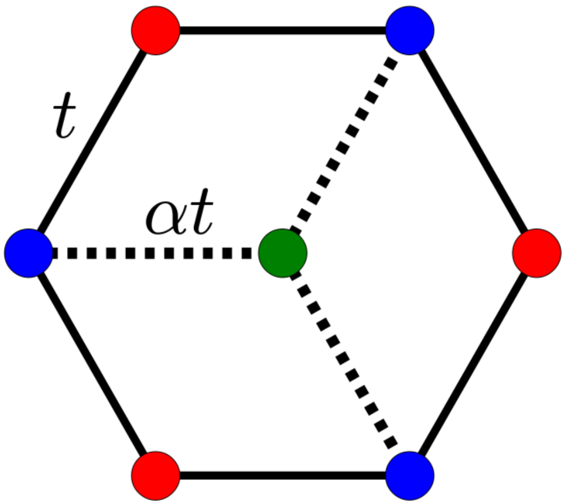

- 2D lattice with variable hopping parameter $\alpha \in [0,1]$, allowing continuous tuning between graphene ($\alpha = 0$) and the dice lattice ($\alpha = 1$).

Kane Fermions

- 3D model for zinc-blende semiconductors like $\mathrm{Hg}_{1-x}\mathrm{Cd}_x\mathrm{Te}$
- Large (Δ) and small (E_g) tunable gap parameters

$$\hbar v\begin{pmatrix} 0 & \frac{\sqrt{3}k_-}{2} & 0 & 0 & 0 & 0 & 0 & 0 \\ \frac{\sqrt{3}k_+}{2} & \frac{E_g}{\hbar v} & -\frac{k_-}{2} & -\frac{k_-}{\sqrt{2}} & -\frac{k_z}{\sqrt{2}} & -k_z & 0 & 0 \\ 0 & -\frac{k_+}{2} & 0 & 0 & 0 & 0 & -k_z & 0 \\ 0 & -\frac{k_+}{\sqrt{2}} & 0 & -\frac{\Delta}{\hbar v} & 0 & 0 & -\frac{k_z}{\sqrt{2}} & 0 \\ 0 & -\frac{k_z}{\sqrt{2}} & 0 & 0 & -\frac{\Delta}{\hbar v} & 0 & -\frac{k_-}{\sqrt{2}} & 0 \\ 0 & -k_z & 0 & 0 & 0 & 0 & \frac{k_-}{2} & 0 \\ 0 & 0 & -k_z & -\frac{k_z}{\sqrt{2}} & -\frac{k_+}{\sqrt{2}} & \frac{k_+}{2} & \frac{E_g}{\hbar v} & -\frac{\sqrt{3}k_-}{2} \\ 0 & 0 & 0 & 0 & 0 & 0 & -\frac{\sqrt{3}k_+}{2} & 0 \end{pmatrix}$$

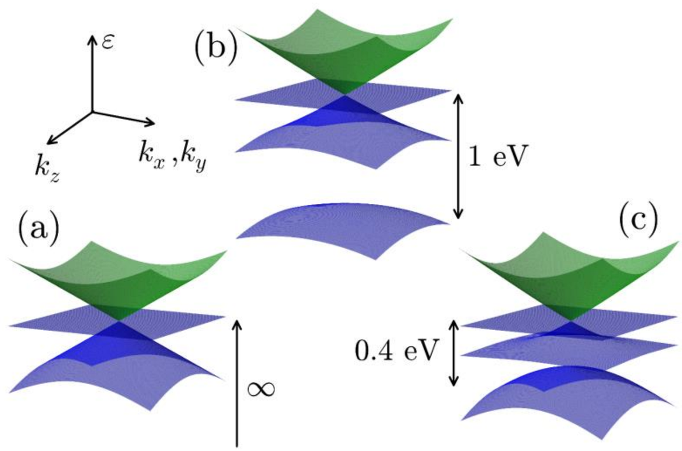

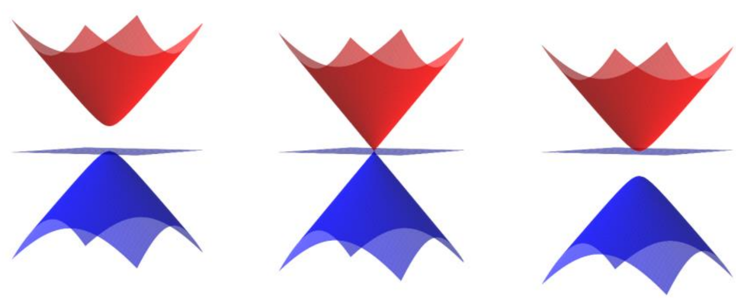

(a) $E_g > 0$ (b) $E_g = 0$ (c) $E_g < 0$

Imaginary Part

- Imaginary part of the polarizability traces out the **particle-hole continuum** (PHC)
- The PHC traces out
- The PHC is greatly extended compared to graphene because of the flat band

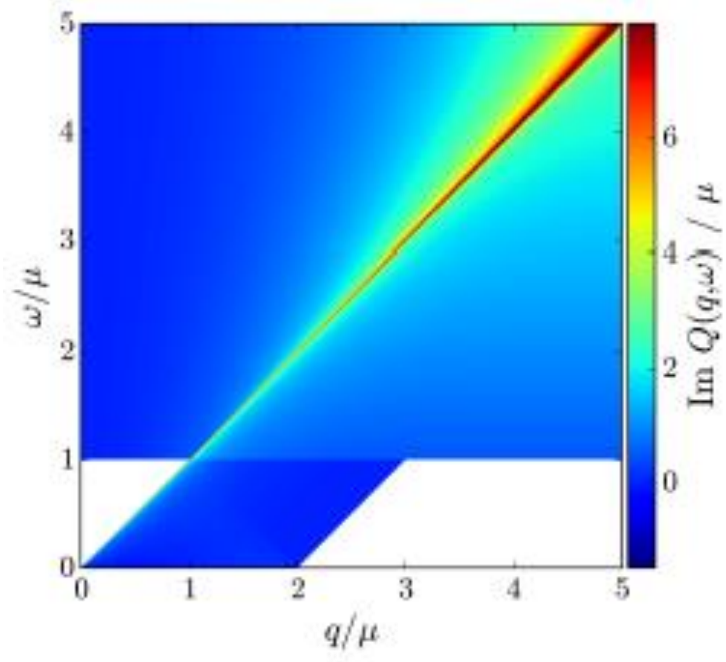

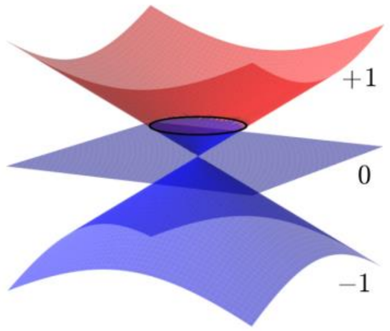

$s = 1$

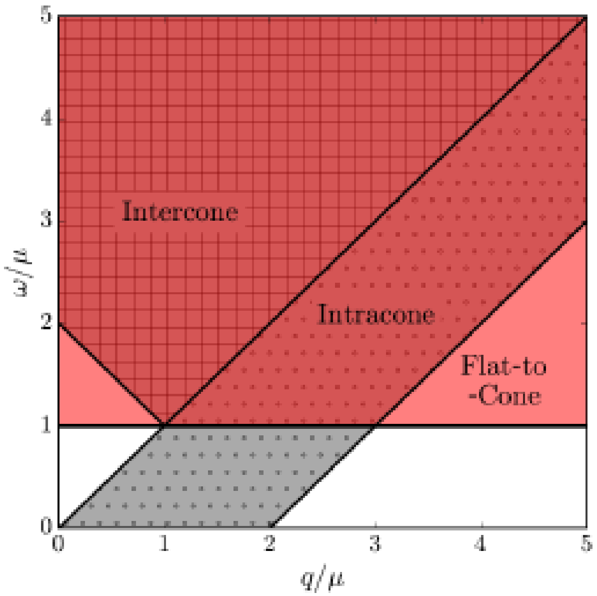

Real Part

- Large screening by flat band evident from the logarithmic divergence in the real part
- Plasmon dispersion is calculated from the real part, showing a pinch point invariant to a change in the dielectric background (substrate)